The coastal landslides of Shetland

Colin K. Ballantyne, Sue Dawson, Ryan Dick, Derek Fabel, Emilija Kralikaite, Fraser Milne, Graeme F. Sandeman, and Sheng Xu

The coastal landslides of Shetland

ABSTRACT Little is known of hard-rock coastal landsliding in Scotland. We identify 128 individual coastal landslides or landslide complexes >50 m wide along the coasts of Shetland. Most are apparently translational slides characterized by headscarps, displaced blocks and/or debris runout, but 13 deep-seated failures with tension cracks up to 200 m inland from cliff crests were also identified. 31 sites exhibit evidence of at least localized recent activity. Landslide distribution is primarily determined by the distribution of coastal cliffs >30 m high, and they are preferentially developed on metasedimentary rocks. Analysis of 16 landslides on Fetlar (NE Shetland) indicates that most are translational dip-slip failures; three represent deep-seated failures; and several exhibit active frontal erosion attributable to basal sapping by storm waves. As these landslides terminate in shallow water, failure was probably initiated when rising sea level resulted in footslope erosion and upslope propagation of instability, causing downslope displacement of landslide blocks on upper slopes. ^{10}Be exposure dating of two headscarps yielded ages of 4.8±0.2 ka and 4.4±0.2 ka, consistent with the onset of footslope erosion as sea level rose. Our results suggest that landslides have played a hitherto undocumented but important role in retreat of cliffed coastlines in Scotland.

KEY WORDS: coastal landslides; rock-slope failure; sea-level rise; arrested translational slides; deep-seated failure; cosmogenic ^{10}Be exposure dating

Introduction

In this paper, the term *landslide* is used to refer to slope failure seated in bedrock, irrespective of the mode of mass movement. Our use of this term therefore incorporates not only rockslides *sensu stricto*, but also major rockfalls, toppling failures, cliff collapses, deep-seated slope displacement, and complex rock-slope failures involving two or more types of movement.

Recent decades have witnessed considerable research into the distribution, age and causes of rock-slope failures in the Scottish Highlands and Hebrides (Ballantyne 1986, 2013; Ballantyne & Stone 2013; Ballantyne *et al.* 2014a, 2014b; Cave & Ballantyne 2016; Jarman 2006, 2007), but current understanding of landslides along the cliffed coasts of Scotland is very limited. For Great Britain as a whole, a literature-based landslide inventory compiled by Jones & Lee (1994) identified over 1300 coastal landslides, but the great majority relate to relatively weak sedimentary rocks or unlithfied sediments, particularly in southern and eastern England. For Scotland north of the Highland Boundary, almost all of the literature on coastal landslides concerns those of the Tertiary Igneous Province on the islands of Skye, Raasay, Mull and Eigg (Anderson & Dunham 1966; Bailey & Anderson 1925; Ballantyne 2016; Godard 1965; Lee 1920; Richards 1971). These landslides involve deep-seated (often rotational) failure of Jurassic sedimentary rocks, usually under stacked Palaeogene lavas, and are therefore structurally and lithologically unrepresentative of coasts elsewhere in Scotland.

There is also a dearth of information on the age of coastal landslides in Scotland. Several authors have noted evidence of recent small-scale movements of some associated with Palaeogene igneous rocks on Skye, Mull and Arran (Anderson & Dunham 1966; Bailey & Anderson 1925; Worth 1956). Richards (1971) investigated the relationships between coastal landslides in the Inner Hebrides and raised shorelines. He found that some apparently pre-date Lateglacial shorelines, implying that failure occurred fairly soon after ice-sheet deglaciation, whereas some pre-date only the highest Holocene shorelines, implying failure during the Lateglacial or early Holocene; others appear to be of more recent (mid to late Holocene) age.

To investigate the nature and distribution of coastal landslides outside the Tertiary Igneous Province we selected the Shetland Isles for analysis, primarily because of the wide range of rock types present (Mykura 1976) and also because the Shetland coastline supports extensive areas of high sea cliffs (Flinn 1974). The aims of the research reported here are (1) to establish the

URL: http://mc.manuscriptcentral.com/rsgj E-mail: crw2@st-andrews.ac.uk dwc3@st-andrews.ac.uk

distribution of moderate- to large-scale landslides on the coasts of Shetland and controls on their distribution, and (2) to investigate in greater detail the nature, characteristics, age and evolution of a subset of the Shetland landslides, through field investigations of those located along the west coast of Fetlar, in NE Shetland.

Shetland: location, geology and Quaternary history

The Shetland archipelago (59°51'–60°51'N; 0°46'–1°46'W; Figure 1) represents the northernmost part of the British Isles. The largest island (Mainland) is deeply indented by inlets and can be subdivided into NW Mainland (west of Sullom Voe), the Walls Peninsula in the west, south Mainland (south of Lerwick) and central Mainland (north of Lerwick). To the NE of Mainland lie the large islands of Yell, Unst and Fetlar (Figure 1) and numerous smaller islands and skerries lie offshore from Mainland. Almost all of Shetland lies below 300 m OD.

Apart from a relatively limited outcrop of basement gneiss of probable Lewisian age, Shetland consists of mainly ancient sedimentary rocks that were metamorphosed and intruded by igneous rocks during the Caledonian Orogeny, and of Devonian sedimentary and volcanic rocks that were emplaced and folded during the final stages of that orogeny (Mykura 1976; Mykura & Phemister 1976). As in the Scottish Highlands, the metasedimentary rocks that underlie most of Shetland (Figure 1) are highly variable in composition and include impure quartzites, gneisses, psammites and pelites. The intrusive complexes are primarily granitic, the sedimentary sequences are dominated by sandstones, often steeply inclined by later folding, and the limited outcrop of volcanic rocks in western Shetland comprises basalts, andesites, rhyolites and ignimbrites with interbedded tuffs and agglomerates. In Unst and Fetlar, a thrust fault separates the metasedimentary sequence from an ophiolite complex of obducted oceanic crust of variable composition, including layers of metaharzburgite, metadunite, metagabbro, phyllite and, in NE Unst, granitic rock (Flinn 2014).

Shetland was completely ice-covered during the last (Late Devensian) glacial maximum of ~27–19 ka. Interpretation of events during this period has polarized around two viewpoints: (1) that the archipelago was over-run by ice moving westwards from the North Sea Basin, and developed an independent ice cap only during ice-sheet retreat (Carr & Hiemstra 2013; Clark *et al.* 2012; Golledge *et al.* 2008), and (2) that Shetland nourished an independent ice cap that persisted throughout the last glacial maximum (Flinn 1977, 1978, 2009). Review of the

literature and field evidence by Hall (2013) strongly supports the latter view. Basal radiocarbon ages from sites on Shetland imply that most of the archipelago was deglaciated between ~17 ka and ~16 ka (Ballantyne & Small 2018). Shetland therefore experienced severe periglacial conditions both during the final period of ice-sheet deglaciation (~17–16 ka to ~14.7 ka) and the Loch Lomond (Younger Dryas) Stade of ~12.9–11.7 ka. During these periods permafrost existed down to sea level and mean annual air temperatures at sea level fell to -6°C or lower (Ballantyne 2018). During much of the Holocene (~11.7 ka to the present) climatic conditions were similar to now, though 'average' temperatures may have oscillated by up to ± 2°C over decades or longer (Briffa & Atkinson 1997).

Throughout the Holocene, sea level has been rising around the coasts of Shetland (Bondevik *et al.* 2005; May & Hansom 2003; Shennan & Horton 2002; Figure 2). Flinn (1964, 1969, 1974, 1977, 2014) has described the characteristics of the Shetland coastline, drawing a distinction between an 'inner coast' of valleys and low-lying areas that have been progressively drowned by Holocene sea-level rise and an 'outer coast' of rock cliffs. He inferred that the present cliffs originated as pre-Pleistocene landforms that have experienced very slow retreat due to wave erosion and resultant cliff collapse during the Quaternary as sea levels fluctuated. He noted that although some cliffs plunge to depths of up to 80 m, in many cases there is a distinct break of slope at or just below the present intertidal zone, with the nearshore rockhead sloping away from the base of cliffs at gentle gradients of around 6°, though rock platforms produced by cliff retreat are generally narrow and localized, and raised beaches are absent. An implication of the basal break of slope at the foot of many Shetland cliffs is that such cliffs may have terminated downslope on dry land above the intertidal zone throughout much of the early and middle Holocene, when sea level was lower than now (Figure 2) and hence were not subject to basal erosion by wave action during this period. Alternatively, the gently-sloping rock ramp in the nearshore may at least in part be the product of renewed coastal erosion and cliff retreat since deglaciation.

The present tidal range around the coasts of Shetland is amongst the lowest in the British Isles (0.75–1.0 m; Clayton *et al*. 2003), implying that wave action is normally limited to a narrow zone at the foot of cliffs. However, the outer coasts of Shetland are exposed to storm waves that rise high above the intertidal zone, particularly on the Atlantic coast, and these have been shown to overtop coastal cliffs up to 40 m high, quarrying angular boulders from cliff crests and depositing these as ridges or spreads of coarse debris inland from the cliff top (Hall *et al.* 2006,

2007; Hansom & Hall 2009). Such cliff-top storm deposits, however, are limited to plunging cliffs that terminate in deep water, as storm wave heights are reduced where cliffs terminate at a basal break of slope.

Distribution and characteristics of coastal landslides on Shetland

Current information on coastal landslides on Shetland is limited: the National Landslide Database of the British Geological Survey records only eight coastal landslides on the archipelago and provides only locational information for these.

Methods

The distribution of coastal rock-slope failures on Shetland was assessed by mapping the sites of all landslides with headscarp or failure-plane widths greater than 50 m (across-slope) using high resolution Google Earth™ imagery, which permits both vertical and oblique visualization from all aspects. Diagnostic characteristics used to identify landslide sites included arcuate, irregular, trapezoidal or V-shaped headscarps, planar or stepped failure planes, downslope-displaced blocks located seaward of headscarps, accumulations of displaced blocks or large boulders on steep coastal slopes or at the foot of cliffs, and tension cracks or scarplets parallel to the crest of cliffs or steep coastal slopes (Figure 3). Equivocal or dubious sites were excluded, as were numerous minor coastal slope failures and rockfall sites less than 50 m wide. Moreover, the coastal cliffs and steep coastal slopes of Shetland are indented by numerous inlets (geos), often arcuate in planform. Some of these probably represent landslide sites but were not included in the inventory unless additional evidence (particularly displaced bedrock blocks) is present. Our inventory of sites is therefore conservative; other possible landslide sites occur along the Shetland coastline but have not been recorded here. A further complication is that at a number of coastal locations a complex of two or more conjoint headscarps or failure planes occurs, and it proved difficult to decide whether these represent a single landslide or multiple landslides, possibly of different age. Such sites were identified as landslide complexes and recorded as a single site, though the number of apparently independent slides within each complex was noted. The outlying islands of Foula and Fair Isle were not included in our survey, though both exhibit evidence for coastal landsliding.

All coastal landslide sites satisfying the diagnostic criteria outlined above were plotted on 1:25000 Ordnance Survey maps. For each site we recorded grid reference and underlying

lithology: metasedimentary rocks, granitic rocks, sandstones, basement gneiss, volcanic rocks and ophiolite complex rocks. We also recorded maximum headscarp height above present sea level, maximum across-slope width, slope aspect and evidence for recent activity in the form of fresh scars, scarps or debris runout. Although the nature of rock-slope failure could not always be assessed from the Google Earth™ imagery, most sites have the characteristics of translational (slope-parallel) rockslides or cliff collapses, locally modified by later minor slides or rockfall, or by frontal erosion. At a small number of sites, however, deep-seated displacement of large rock masses was evident in the form of arrays of across-slope tension cracks or scarplets located 60–200 m inland from the crests of cliffs. Such sites were recorded as deep-seated gravitational slope deformations (DSGSDs).

Results

A total of 128 landslide sites were identified around the coast of Shetland using the criteria outlined above: 28 on Unst, 16 on Yell, 23 on Fetlar, 36 on NW Mainland, 11 on the Walls Peninsula, 13 on south Mainland and one on the island of Bressay, east of Lerwick (Figure 4). If conjoint failure scarps within landslide complexes are counted as individual landslides, the total rises to just over 200, though a precise figure cannot be given as the number of individual failure scarps distinguishable in some complexes could not be determined.

With the exception of DSGSDs (where tension cracks, scarplets and/or large displaced rock masses occur inland and upslope from cliff crests) all but two of the recorded landslide sites represent full-slope failures that extend to, or nearly to, the crest of coastal cliffs, so that landslide height is effectively almost identical to cliff height. Minimum and maximum landslide heights range from ~30 m to ~275 m, with a median height of 80 m and interquartile range of 50–105 m; only small slope failures and localized rockfall were observed on cliffs < 30 m high. This limit accounts for the absence of recorded landslides along the generally low-lying coast of central Mainland, where coastal bluffs and cliffs rarely exceed 30 m in altitude. Excluding landslide complexes and DSGSDs, the across-slope widths of recorded individual landslides ranges from 50 m to 570 m, though, only four exceed 300 m; median width is 120 m and the interquartile range is 80–150 m. Some landslide complexes and DSGSDs are much wider: the cliffs of Valla Kames in NW Mainland [HU 300869] are interpreted as a landslide complex ~1120 m wide and up to 165 m high, and the adjacent Stonga Banks landslide [HU 293856] is a complex DSGSD ~805 m wide and up to 235 m high, with an array of tension cracks extending ~200 m inland from the crest of the cliff; this is probably the largest coastal landslide on

Shetland. Individual landslides in metasedimentary rocks tend to increase in width with increasing height, but those classified as DSGSDs tend to be markedly wider than those that have involved translational sliding and slumping of blocks from the cliff crest (Figure 5).

The primary control on the distribution of the recorded landslides is the distribution of cliffs >30 m high; most lower cliffs exhibit no evidence of collapse, or only small slides or rockfalls. Although landslides occur on cliffs at all aspects, 60% have westerly aspects (SW, W and NW; Figure 6), but as a similar percentage of cliffs > 30 m high also have westerly aspects, this bias probably reflects the distribution of high coastal cliffs. It is notable, however that only 28% of recorded landslide sites occur in relatively sheltered locations where fetch is limited across adjacent sounds, notably those on the east coast of NW Mainland facing Yell Sound, and those on the west coast of Fetlar facing Colgrave Sound (Figure 4). Almost all other recorded landslide sites are open to the Atlantic Ocean or North Sea and thus exposed to powerful storm waves.

Classification of landslides by major lithological groups (metasedimentary rocks, granitic rocks, sedimentary rocks (sandstones), ophiolite complex rocks, basement gneiss and volcanic rocks) suggests that lithology exercises an important control on their distribution. The majority (71.9%) of recorded landslides or landslide complexes are seated on metasedimentary rocks (Table 1). This predominance might be expected given the extensive coastal outcrop of metasedimentary lithologies (Figure 1). Much of the coastline underlain by metasedimentary rocks is low-lying, however, and not susceptible to slope failure. When the frequency of landsliding on different lithologies is compared with that of 'potential' landslide sites represented by cliffs > 30 m high (Table 1), it is clear that landsliding on metasedimentary rocks is over-represented and that for all other lithologies is under-represented. Collectively, the observed frequency for all lithologies differs from the expected frequency ('potential' sites) at $p < 0.001$ (χ^2 test), implying that metasedimentary rocks have exhibited a significantly greater propensity for failure than others represented in the coastal cliffs of Shetland, and it is notable that all but two of the 13 landslides recorded as DSGSDs occur in metasedimentary rocks. Although not quantified, we also observed that cliffs on other lithologies tend to be steeper than those on metasedimentary rocks, also suggesting that the latter have been more prone to landsliding.

The occurrence of most coastal landslides on Shetland on metasedimentary rocks echoes the situation in the mountainous parts of the Scottish Highlands, where the great majority of rock-

slope failures have also occurred on Neoproterozoic metasedimentary of Moine or Dalradian age, particularly schists (Ballantyne 1986; Cave & Ballantyne 2016; Jarman 2006). Similarly, Crosta *et al.* (2013) have shown that DSGSDs in the Alps occur preferentially on foliated metamorphic rocks, and Saintot *et al.* (2011) have demonstrated that large rock-slope instabilities in western Norway are mainly developed in phyllites, schists and foliated gneisses. The high incidence of failure on metasedimentary rocks in the Highlands was attributed by Watters (1972) and Holmes (1984) to their inherent weakness, relatively low friction angles and propensity for failure at sites where bedding or foliation dips out of the slope, forming potential failure planes. It is likely that similar factors are responsible for the relatively high density of coastal landslides on metasedimentary rocks in Shetland.

Recent activity in the form of fresh scarps, areas of stripped rock and accumulations of fresh debris were recorded at 31 landslide sites (24%). In most cases this represents superficial rockfall or shallow sliding of debris from cliffs or the fronts of detached landslide blocks (Figure 3) but evidence of recent large-scale failure was detected at three sites, the most prominent being the Saito landslide in northern Unst (Figure 3c), where a fresh headscarp and sidescarp indicate recent slumping of landslide blocks across a 200 m wide section of coastline.

The west Fetlar coastal landslides: setting

Field-based investigations of a subset of coastal landslides were made along the west coast of Fetlar in NW Shetland (60.62°N; 0.87°W; Figures 1 and 4). The west Fetlar landslides occupy a 2.8 km long stretch of cliffed coastline between Corbie Head [HU 582914] and Bresdale [HU 598888]. The cliffs decline gradually in altitude southwards from 80–95 m OD to 30–50 m OD, and are underlain by Valla Field Schists of Dalradian age (Flinn 2014). In this area these are mainly coarse pelites interleaved with locally dominant bands of orthoquartzite and impure quartzite up to ~4 m thick. These rocks are extensively fractured and dip steeply (up to 45°) westwards to southwestwards, outwards from the cliffs towards the sea.

The west coast of Fetlar is separated from the adjacent island of Yell by the 5 km wide Colgrave Sound, which is less than 40 m deep 1.5 km offshore from west Fetlar and shallows eastwards, so that the Fetlar landslides now terminate in tidewater no more than a few metres deep (Dick 2015). Shingle beaches occupy small inlets at the northern end [HU 584914], Grunni Geo [HU 592902] south of Bratta Stack [HU 594889]. Though exposed shore platforms are absent,

there is a marked break of slope at the foot of the cliffs, either at or a few metres below present sea level, and large submerged blocks of landslide debris are visible on the sea floor just below the intertidal zone. During the early Holocene, when sea level was at least 10–15 m (and possibly as much as 30 m) below present (Figure 2), the shoreline must have been located offshore so that the west Fetlar cliffs mainly terminated on land. This scenario is consistent with Flinn's (2014) view that the coastal cliffs of northern Shetland are essentially inherited features that have merely been 'trimmed' by wave action and slope processes during the Holocene. Moreover, the coastline of west Fetlar is relatively sheltered from high-energy storm waves. Westerly fetch is limited to no more than 5 km by the width of the Colgrave Sound, and southerly fetch is limited to ~25 km by the island of Whalsay. As wave height is roughly proportional to the square root of fetch (Sverdrup, 2006), this coastline is unlikely to have experienced attack by extremely high-energy waves such as those that affect the western coasts of Shetland, which are exposed to the Atlantic Ocean.

Geomorphology of the west Fetlar landslides

Landslides extend almost continuously along the studied area, making it one of the densest concentrations of coastal landsliding on Shetland (Figure 4). Fifteen individual landslide sites and one landslide complex were identified and numbered (NW to SE) F1–F16.

Most of the west Fetlar landslides (F4–F12 and F14) share common characteristics. These have generally well-defined headscarps up to ~10 m high, downslope of which are one or more displaced landslide blocks (Figures 7–9). At some sites these form a stepped profile, but at others they are represented by small upslope-facing scarps (antiscarps). Although the arcuate or bowl-shaped planform of some of these landslides (for example F5, F6 and F7) appears consistent with rotational sliding, we found no convincing evidence for back-tilting of landslide blocks indicative of an underlying curved failure plane. The alignment of displaced blocks (Figure 9d,e) is consistent with those of arrested dip-slip translational (slope-parallel) sliding along steep bedding or foliation planes, or joint sets guided by these structures. This interpretation is supported by the presence at the toe of several of the landslides of a steeply seaward-dipping (~35–45°) bedrock ramp that indicates the structural trend under the slipped masses. It is also supported by the configuration of site F1 (Figure 9a) and the southern margin of F4, which consist of steep, approximately planar surfaces flanked by cliffed sidewalls up to 30 m high, and are interpreted as the sites of former structurally-guided translational slides that

terminated below present sea level. A further example of a similar failure plane occurs at the northern end of site F15; this site is interpreted as a landslide complex that incorporates two or possibly three conjoined failure zones. Site F3 appears to represent a simple arrested translational rockslide, but here the headscarp is degraded and indistinct, and there is no clear evidence of block detachment. At two sites where the headscarp is exposed (F4 and F8) failure appears to have taken place along the steeply-seaward-inclined contact between quartzite and the underlying phyllites, but similar contacts could not be detected elsewhere because of lack of exposure.

Three of the Fetlar landslides (F2, F13 and F16) are interpreted as deep-seated failures (DSGSDs) on the grounds that scarps or tension cracks indicative of block detachment occur 100–130 m inland from the cliff crest (Figures 7 and 8). These sites exhibit contrasting degrees of detachment. Displacement at site F2 (Figure 9b) is marked by an irregular headscarp 315 m long that increases in height southward and marks the landward limit of a complex array of detached blocks that have moved both vertically and horizontally from the headscarp; some are tilted slightly seaward, producing small antiscarps. The inland extent of F13 is marked by peat-covered tension cracks and scarplets (Figure 9f) that define a block 295 m wide, which appears to have moved a very limited distance both horizontally and vertically, without fragmenting into individual detached blocks. Finally, F16 is defined only by tension cracks, some of which are occupied by small streams. These fractures indicate partial detachment of a block 310 m wide with very limited or no vertical or lateral displacement. Degree of displacement appears to reflect the height of the blocks: the highest part of the F2 headscarp reaches 93 m OD, the rearmost tension cracks at F13 occur at 80 m OD, and the tension cracks defining the landward extent of F16 are at only 45 m OD.

Most of the west Fetlar landslides have experienced post-sliding modification, some of it recent. This takes two forms. Small-scale collapse of headscarps (Figure 9e) or the seaward edges of slipped blocks (Figure 9c) has resulted in deposition of coarse rockfall debris at sites F5 and F8. The freshness of such debris at these sites indicates recent scarp collapse, unrelated to the main period of landsliding, but older rockfall debris is also evident at some other sites. Also common is evidence for erosion of the foot zone at several sites (F6, F7, F9, F10, F14, F15), including the three deep-seated failures (F2, F13 and F16). This takes the form of fresh scars extending up the face of the landslides from sea level, and indicates superficial failure (rockfall, debris fall and shallow sliding failure) caused by recent erosion of footslopes by storm wave action. However,

we observed no evidence of wave-eroded notches at the foot of any of the landslides: some terminate at an intertidal or sub-intertidal break of slope, and the base of others is represented by a steep, structurally-controlled bedrock ramp that has been stripped of sediment cover by wave action.

Dating of the west Fetlar landslides and implications for causes of failure

The preservation of distinct headscarps and displaced blocks (Figures 7–9) demonstrates that the west Fetlar landslides occurred after deglaciation at ~17–16 ka, though it is possible that the subdued landslide scar at F3 may pre-date over-running by glacier ice at the last glacial maximum. To assess the timing of landsliding, we collected samples for cosmogenic ^{10}Be exposure dating from cliffed headscarps at sites F4 and F8. At both sites, two bedrock samples were chiseled from impure quartzite at the top of small rock steps near the foot of the headscarp, and topographic shielding (which reduces exposure to cosmic radiation) at each sampling site was measured by compass and abney level. Site and analytical details are given in Table 2.

Exposure ages for each sample were calculated using versions 2.3 and 3 of the online exposure age calculators formerly known as the CRONUS-Earth online exposure age calculators (Balco *et al.* 2008) and CRONUScalc 2.0 (Marrero *et al.* 2016) and two ^{10}Be production rates: the Loch Lomond production rate (LLPR), based on ^{10}Be concentration in samples from boulders on an independently-dated moraine of Younger Dryas age near Loch Lomond in the Midland Valley of Scotland (Fabel *et al.* 2012) and the global production rate of Borchers *et al.* (2016). We assume post-exposure erosion (ε) of sampled surfaces of 1 mm ka^{-1}; assumption of ε = 0 reduces ages by < 0.4% and assumption of ε = 2 mm ka^{-1} increases ages by < 0.4%. We employed Lm scaling of the CRONUS calculator to determine ages, as this has been employed in previous research on the ages of rock-slope-failures in Scotland (Ballantyne *et al.* 2014a, b). Use of an alternative (LSD) scaling scheme with LLPR produced ages ~100 years younger, and use of SA scaling with CRONUScalc 2.0 produces ages 210–280 years younger.

The results (Table 3) are therefore reasonably robust irrespective of the assumptions made in their calculation, and are remarkably consistent for both samples from each site. They indicate that exposure of the headscarps occurred at ~4.5 ± 0.2 ka (F4) and ~4.8 ± 0.2 ka (F8). The two ages are not significantly different (two-sample difference of means test) and could represent either synchronous failure or failure separated by a few centuries.

The timing of these two landslides allows several possible causes of failure to be eliminated. As they occurred over 11,000 years after deglaciation, they are clearly unrelated to glacial debuttressing (removal of supporting ice from cliffs during ice-sheet retreat) or generation of high cleft-water pressures during deglaciation. Similarly, thaw of permafrost ice in joints can be ruled out as a trigger, as permafrost disappeared from low ground in Scotland shortly after the Lateglacial-Holocene transition at ~11.7 ka (Ballantyne 2018). Various authors have shown that coastal rock-slope failure may been triggered by seismic events (e.g. Komar & Shih 1993; Hapke & Richmond 2002), and Ballantyne *et al.* (2014a,b) have demonstrated a temporal correspondence between the timing of postglacial rock-slope failure and the rate of glacio-isostatic crustal uplift in Scotland, suggesting that many landslides in the Highlands and Hebrides were triggered by earthquakes. However, by ~5 ka rates of crustal uplift had relaxed to low levels (< 5 mm a^{-1}) at locations close to the centre of uplift (Firth & Stewart 2000), and were probably much lower in peripheral areas such as Shetland. It therefore seems extremely unlikely that earthquakes triggered slope failure at sites F4 and F8. It is also notable that of 20 dated inland rock-slope failures on terrain deglaciated by the last ice sheet and not subsequently reoccupied by glacier ice, all but one occurred prior to ~11.7 ka and all occurred before ~6.1 ka (Ballantyne *et al.* 2014a). The timing of headscarp exposure at sites F4 and F8 indicates that these landslides occurred much later, suggesting that different factors controlled the timing and trigger of failure at these sites.

Interpretation

The geomorphological observations outlined above suggest that most of the west Fetlar landslides are dip-slip translational slides that have involved arrested downslope displacement of detached blocks of rock on upper slopes, apparently along steeply-dipping bedding planes, or major joints sloping steeply seaward. At three sites (F1 and parts of F4 and F15) steep rectilinear slopes with prominent sidewalls are interpreted as marking the sites of translational slides that terminated offshore. Three sites are interpreted as deep-seated failures, with the degree of block detachment being related to height above sea level. Many 'primary' landslides have experienced subsequent modification by erosion of footslopes leaving fresh scars, and some exhibit evidence of scarp collapse and rockfall farther upslope.

Our dating evidence shows that two of the west Fetlar landslides occurred in the mid to late Holocene (~4.5 and ~4.8 ka), and though the representativeness of these ages is not known, they demonstrate that at least localized failure occurred at these times, and suggest that the controls on coastal landsliding differ from those affecting inland rock-slope failures. A probable explanation is that coastal landsliding represents a response to storm wave erosion acting at the foot of cliffs. As noted earlier, the west Fetlar landslides terminate downslope at the intertidal zone or in shallow water no more than a few metres deep, implying that the antecedent (pre-failure) slope terminated above sea level during the early Holocene. The sea-level curve for Shetland (Bondevik *et al.* 2005; Figure 2) implies that at ~6.5 ka, sea-level was at least 10–16 m below present, implying that at that time much of toe of the antecedent slope was above sea level. By ~4.5 ka (the approximate timing of the landslides at F4 and F8) sea-level was only 4–5 m below present, implying that by this time much of the foot of the antecedent slope lay within, just above or just below the intertidal zone. Moreover, after ~4.5 ka the rate of sea-level rise slowed, so that the critical zone for wave erosion of the foot of the slope rose only very slowly, at an average rate of only 1 m ka^{-1} (1mm per year), thus prolonging wave action within a narrow zone at the foot of the cliffs (Kline *et al.* 2014; Trenhaile 2002a,b, 2010). These considerations suggest that coastal landsliding at this site was initiated by rising sea level allowing storm waves to access the foot of the antecedent slope, after which the critical zone of slope-foot wave erosion rose only very slowly, permitting prolonged wave action to destabilize the slope. An analogous situation has been described for landslides on the Isle of Wight by Hutchinson *et al.* (1991), who attributed renewed movement of ancient landslide blocks to rising Holocene sea level and consequent marine erosion. Similarly, Pánek *et al.* (2018) have shown that major rockslides along the Crimean coast were associated with major transgressive episodes affecting the Black Sea.

Storm waves impacting the foot of cliffs exert both hydraulic force through the processes of wave quarrying, water hammer (shock pressure generated by breaking waves) and air compression in open fractures, as well as mechanical abrasion where coarse sediment is available at the cliff foot (Adams *et al.* 2005; Sunamura 1992; Trenhaile 1987; Williams *et al.* 1993). Most models of sea-cliff retreat, however, are based on the assumption that this occurs through undercutting (notch development) and subsequent collapse of the undercut cliff (e.g. Ashton *et al.* 2011; Belov *et al.* 1999; Kline *et al.* 2014) and take no account of structural configuration. Modelling of the effects of rock structure by Allison & Kimber (1998), however, has shown that the nature of sea-cliff failure is strongly determined by the dip of bedding and

the strike and dip of principal joint sets. In particular, their model indicates that steeply outward dipping joints or beds are dominated by translational sliding failure, with displaced blocks resting on the upper slope and cliff collapse on the lower slope. This situation corresponds closely with the configuration of most of the west Fetlar landslides (F4–12 and F14). Detailed field studies, moreover, have shown that sea cliffs are also subject to small-scale iterative modification through overhang collapse, spalling, fragmentation, rockfall and debris fall triggered by processes such as frost action, stress release and high cleft-water pressures (Allison 1989; Lim *et al.* 2010; Trenhaile 1997). Such a situation corresponds to that of the active footslope erosion evident at the distal end of some west Fetlar landslides (F2, F6, F7, F9, F10, F13–16; Figures 7 and 8).

Based on our knowledge of the morphology and structure of the arrested translational landslides on the west Fetlar coast (Figure 8), the timing of Holocene sea-level rise (Figure 2) and the mid-to-late Holocene ages of the translational failures at sites F4 and F8 (Table 3), we propose a sequence of postglacial landslide evolution (Figure 11). We take as a starting point (Figure 11a) a 45° structurally-controlled bedrock slope terminating above sea-level, and buttressed by a talus comprising Lateglacial rockfall debris (Hinchliffe & Ballantyne 1999, 2009). By mid-to-late Holocene (Figure 11b), rapidly rising sea level permits storm waves to access the foot of the slope, removing and comminuting the basal talus and eroding the slope foot, eventually triggering sliding failure of the lower slope along a failure plane guided by the structural dip. Subsequently (Figure 11c), instability progressively propagates upslope, causing downslope displacement of landslide blocks and development of the stepped profile that characterizes many of the west Fetlar landslides. The rate of upward progression of instability is not known; this may have occurred concurrently with failure of the lower slope, or delayed by centuries or millennia. Removal of the support of the lower slope segment must have increased the shear stress operating along discontinuities in the upper slope, inducing progressive brittle failure ('static fatigue'). At sites where there is evidence of full-slope translational sliding (F1, the southern part of F4 and the northern part of F15) it is likely that failure of the entire slope was instantaneous, generating catastrophic slides that terminated offshore. Conversely, displaced upper slope blocks are interpreted as arrested sliding failures, suggesting that these moved more gradually, stabilizing as asperities across the underlying shear planes 'locked', reducing or terminating movement. Movement may also have been aided by enhanced cleft-water pressures, which would have had the effect of reducing the effective normal stress holding blocks in place. At present (Figure 11d), slipped blocks appear stable and the foot of many landslide sites is

represented by a structurally controlled bedrock ramp. However, as noted above, the footslope zones of several landslides exhibit recent erosion, which is inferred to represent rockfalls, debris falls and shallow slides triggered by storm wave erosion and subaerial processes (*cf.* Lim *et al.* 2010; Trenhaile 1997). Retreat of eroded footslopes may potentially trigger renewed gradual or catastrophic displacement of displaced blocks perched above the zone of active erosion.

The reconstruction outlined in Figure 11 appears to account for the present morphology of most of the west Fetlar landslides, but not the evidence for deep-seated movement evident at sites F2, F13 and F16 (and other sites along the Shetland coastline). A possible explanation for such deep-seated movement is coastal slope retreat or steepening. Beneath flat land inland from the coastal slope the principal stress (overburden weight) acts vertically. As the coastal slope is approached, however, the principal stress becomes progressively curved towards the slope (Figure 12). It has been shown that in an isotropic medium, a potential shear surface develops at angle (α) to the direction of principal stress, expressed as $\alpha = [45° + (\phi/2)]$, where ϕ is the angle of internal friction, producing a curved potential shear plane under the slope and adjacent ground (e.g. Jones & Lee 1994; Lambe & Whitman, 1969; Figure 12). Retreat of the slope face (by translational landsliding, cliff collapse or coastal erosion), however, has the effect of both debuttressing the rock mass farther inland and increasing the average slope of the shear plane, potentially initiating deep movement. Rising sea level may also have contributed to rock-mass shift by raising the water table, thereby increasing cleft-water pressures that reduce the effective normal stress acting along the shear plane. The steeply-dipping rocks of west Fetlar, however, are strongly anisotropic, and here rock-mass shift is likely to have occurred along pre-existing structural discontinuities (bedding planes and related joint sets), rather than simple rotational movement along a deep-seated failure plane. Thus it is possible that erosion and retreat of coastal slopes (and possibly rising sea level) changed the state of stress within coastal rock masses, permitting deep-seated rock-mass movement 100–200 m inland from cliff crests. This interpretation appears consistent with the relationship between slope height and degree of deep-seated displacement at sites F2, F13 and F16, as the curvature of principal stress increases with slope height.

Discussion and wider implications

As outlined in the introduction, studies of coastal landsliding in Scotland have been almost exclusively limited to accounts of large, deep-seated failures in the Tertiary Volcanic Province of the Inner Hebrides. Here we demonstrate that moderate- and large-scale landslides have played an important role in postglacial modification of coastal cliffs > 30 m high on a range of lithologies in Shetland, and that such landslides have preferentially occurred in metasedimentary rocks. Our results suggest that the role of landsliding in postglacial rock-coast evolution in Scotland has been much greater than the present dearth of research suggests, particularly as many rock coasts in Scotland north of the Highland Boundary are underlain by dipping metasedimentary rocks of Moine and Dalradian age, similar to those of Shetland.

Shetland is atypical, however, in that the archipelago has experienced apparently uninterrupted (though slowing) sea-level rise throughout the Holocene, a characteristic that it shares only with other peripheral areas such as Caithness, Orkney and the Outer Hebrides (Dawson & Smith 1997; Dawson & Wickham-Jones 2007; Jordan *et al.* 2010). Analysis of the nature and distribution of coastal landslides in these areas would be rewarding, particularly as they are underlain by different rock types: gently-dipping sandstones (Orkney and Caithness) and gneiss (Outer Hebrides). Other Scottish coasts experienced initial submergence but net Holocene emergence, often leaving relict cliffs isolated from the sea by raised shorelines, and in such locations evidence of landsliding may be limited to such former sea cliffs. Even in areas of net Holocene emergence, however, sea cliffs are widespread along the Scottish coast, and the influence of landsliding (as opposed to cliff collapse and incremental rockfall) in cliff evolution remains to be established.

Our study of the west Fetlar landslides indicates that the majority are essentially dip-slip translational slides, with a steep frontal bluff succeeded upslope by displaced landslide blocks. On Fetlar, his configuration appears to be conditioned by the steep seaward dip of the underlying metasedimentary rocks, and corresponds closely with model predictions (Allison & Kimber 1998). Many other coastal landslides on Shetland have a similar morphology, though it remains to be determined if this also occurs independently of lithology and underlying structural configuration, or whether it is conditioned primarily by the dip of bedding or that of the principal joint sets (Williams *et al.* 1993). We suggest that large, deep-seated failures (DSGSDs) reflect change in the state of stress due to cliff erosion and retreat, which debuttresses coastal

rock masses and increases shear stress at depth, but the role of rising sea level in raising the water table and reducing effective principal stress is unknown. Such features deserve more detailed investigation.

The mid-to-late Holocene timing of failure at two west Fetlar sites, the evidence for the rate sea-level rise and downslope termination of the west Fetlar cliffs in shallow water suggests that postglacial failure was initiated when rising seas accessed the foot of the cliffs, allowing storm waves to erode the base of the cliffs and thus trigger instability that propagated upslope. Whether this situation is exceptional remains to be determined. Our survey of Shetland landslides, however, indicated that the majority terminate in shallow water, confirming Flinn's (1964, 1969, 1974, 1977) observation that the Shetland sea cliffs often terminate downslope at a shallow break of slope, so that sapping by storm wave erosion affected such cliffs only when rising Holocene sea level accessed the base of cliffs. This scenario, however, is inapplicable in the case of plunging cliffs that extend up to 80 m below present sea level. At such locations storm-waves may have affected coastline evolution during much or all of the period since ice-sheet deglaciation (~17–16 ka), and the timing (and possibly nature) of postglacial landsliding at these sites is likely to differ from those of cliffs that remained above the level of storm wave erosion throughout the early Holocene.

Finally, our survey indicates that some coastal landslides exhibit evidence of recent activity. This mostly takes the form of an actively-eroding footslope, characterized by storm-wave erosion, small-scale collapse, rockfall and debris fall, though some sites also exhibit evidence of recent scarp collapse on upper slopes and three sites on Shetland appear to have experienced more extensive recent failure. These observations imply that future instances of large-scale slope failure triggered by footslope sapping are likely. The hazard posed by future landslides appears limited, however. In part this is because the characteristic mode of failure identified here is arrested translational sliding (block displacement) rather than catastrophic failure, but also because most landslide sites face the open sea, so displacement waves triggered by large catastrophic failures are unlikely to affect settled parts of the archipelago. However, Bondevik *et al.* (2005) have recorded three tsunami layers (sand layers within coastal fen and lake deposits) at various sites on Shetland. The earliest, dated to ~8.1 ka, is attributable to the well-documented Storegga submarine landslide west of Norway (Dawson *et al.* 1988). The two younger tsunami events are estimated to have occurred at ~5.5 ka and ~1.5 ka. Sedimentary evidence for the ~1.5 ka tsunami has been described for Basta Voe on the eastern coastline of

the adjacent island of Yell, facing the west Fetlar cliffs (Dawson *et al.* 2006). The source mechanism for this tsunami has never been established and the possibility that was caused by catastrophic landsliding cannot be ruled out.

Conclusions

1. We have identified at least 128 landslides or landslide complexes around the cliffed coasts of Shetland from the evidence provided by headscarps, detached blocks and runout debris. Most individual sites are less than 300 m wide, and sites >50 m wide appear to be restricted to cliffs >30 m high. The majority of sites involve arrested, apparently translational sliding of landslide blocks, though tension cracks and scarplets up to 200 m from the cliff crest suggest that at least 13 sites involved deep-seated movement.

2. Coastal landslides on Shetland, like major inland rock-slope failures, are preferentially developed on metasedimentary rocks. Much smaller numbers were detected on granitic, sandstone and gneissic rocks, or rocks of the ophiolite complex in Unst and Fetlar.

3. Detailed study of 16 coastal landslides on the west coast of Fetlar indicates that these mainly consist of arrested dip-slip translational slides. We infer that these were triggered by basal sapping of the slope foot and subsequent upslope propagation of instability, causing block displacement on upper slopes. At three sites, deep-seated movement may have been triggered by slope steepening or retreat due to translational sliding or cliff collapse, which altered the state of stress in the adjacent rock mass.

4. The headscarps of two west Fetlar landslides yielded cosmogenic ^{10}Be exposure ages of ~4.5 ka and ~4.8 ka. These ages are consistent with failure occurring after sea-level rise allowed storm waves to access the slope foot. As many Shetland landslides terminate in shallow water, it is likely that Holocene sea-level rise was instrumental in instigating slope failure at such sites.

Finally, this study has demonstrated the potential significance of postglacial landsliding as an agent of coastal retreat and coastline modification along the hard-rock cliffed coasts of Scotland. Further investigation of the role of landsliding on cliffed coasts that are underlain by different lithologies and/or have experienced different histories of sea-level change is likely to provide useful information on the age, nature and significance of coastal landslides, a research field that has hitherto remained untilled.

References

Adams, P. N., Storlazzi, C. D., & Anderson, R. S. (2005). Nearshore wave-induced cyclic flexing of sea cliffs. *Journal of Geophysical Research, 110,* F02002.

Allison, R. J. (1989). Rates and mechanisms of change in hard rock coastal cliffs. *Zeitschrift für Geomorphologie Supplement Band, 73,* 125–138.

Allison, R. J., & Kimber, O. G. (1998). Modelling failure mechanisms to explain rock slope change along the Isle of Purbeck Coast, UK. *Earth Surface Processes and Landforms, 23,* 731–750.

Anderson, F. W., & Dunham, K. W. (1966). *The Geology of Northern Skye.* Memoir of the Geological Survey the United Kingdom (Edinburgh: HMSO).

Ashton, A. D., Walkden, M. J. A., & Dickson, M. E. (2011). Equilibrium responses of cliffed coasts to changes in the rate of sea level rise. *Marine Geology, 284,* 217–229.

Bailey, E. B., & Anderson, F. W. (1925). *The geology of Staffa, Iona and Western Mull*. Memoir of the Geological Survey, Scotland (Edinburgh: British Geological Survey).

Balco, G., Stone, J. O., Lifton, N. A., & Dunai, T. J. (2008). A complete and easily accessible means of calculating surface exposure ages or erosion rates from ^{10}Be or ^{26}Al measurements. *Quaternary Geochronology 3,* 93–107.

Ballantyne, C. K. (1986). Landslides and slope failures in Scotland: a review. *Scottish Geographical Magazine, 102,* 134–150.

Ballantyne, C. K. (2013). Lateglacial rock-slope failures in the Scottish Highlands. *Scottish Geographical Journal, 129,* 67–84.

Ballantyne, C. K. (2016). Rock-slope failures on Skye. In C. K. Ballantyne, & J. J. Lowe (Eds.) *The Quaternary of Skye: Field Guide* (pp. 77–88). London: Quaternary Research Association.

Ballantyne, C. K. (2018). After the ice: Lateglacial and Holocene landforms and landscape evolution in Scotland. *Earth and Environmental Science Transactions of the Royal Society of Edinburgh.* In press.

Ballantyne, C. K., & Harris, C. (1994). *The Periglaciation of Great Britain* (pp. 330). Cambridge: Cambridge University Press.

Ballantyne, C. K., Sandeman, G. F., Stone, J. O., & Wilson, P. (2014a). Rock-slope failure following Late Pleistocene glaciation on tectonically stable mountainous terrain. *Quaternary Science Reviews, 86,* 144–157.

Ballantyne, C. K., & Small, D. (2018). The Last Scottish Ice Sheet. *Earth and Environmental Science Transactions of the Royal Society of Edinburgh,* In press.

Ballantyne, C. K., & Stone, J. O. (2013). Timing and periodicity of paraglacial rock-slope failure in the Scottish Highlands. *Geomorphology, 186,* 150–161.

Ballantyne, C. K., Wilson, P., Gheorghiu, D., & Rodés, À. (2014b). Enhanced rock-slope failure following ice-sheet deglaciation: timing and causes. *Earth Surface Processes and Landforms, 39,* 900–913.

Belov, A. P., Davies, P., & Williams, A. T. (1999). Mathematical modeling of basal coastal erosion in uniform strata: a theoretical approach. *Journal of Geology, 107,* 99–109.

Bondevik, S., Mangerud, J., Dawson, S., Dawson, A. G., & Lohne, Ø. (2005). Evidence for three North Sea tsunamis at the Shetland Islands between 8000 and 1500 years ago. *Quaternary Science Reviews, 24,* 1757–1775.

Borchers, B., Marero, S. M., Balco, G., Caffee, M., Goehring, B., Lifton, N., Nishiizumi, K., Phillips, F. M., Schaefer, J. & Stone, J. O. (2015). Geological calibration of spallation production rates in the CRONUS-Earth project. *Quaternary Geochronology, 31,* 188–198.

Briffa, K. R., & Atkinson, T. C. (1997). Reconstructing Late-glacial and Holocene climates. In M. Hulme & E. Barrow (Eds.) *Climates of the British Isles: Present, Past and Future* (pp. 84–111). London: Routledge.

Carr, S. J., & Hiemstra, J. F. (2013). Sedimentary evidence against a local ice cap on the Shetland Isles at the Last Glacial Maximum. *Proceedings of the Geologists' Association, 124,* 484–502.

Cave. J. A. S., & Ballantyne, C. K. (2016). Catastrophic rock-slope failures in NW Scotland: quantitative analysis and implications. *Scottish Geographical Journal*, *132,* 185–209.

Clark, C. D., Hughes, A. L. C., Greenwood, S. L., Jordan, C., & Sejrup, H. P. (2012). Pattern and timing of retreat of the last British-Irish Ice Sheet. *Quaternary Science Reviews, 44,* 112–146.

Clayton, K. M., Bird, E. C. F., & Hansom, J. D. (2003). The geomorphology of the coastal cliffs of Great Britain. In V. J. May, & J. D. Hansom (Eds.) *Coastal Geomorphology of Great Britain* (pp. 31–53). Geological Conservation Review Series No 23. Peterborough: Joint Nature Conservation Committee.

Crosta, G.B., Frattini, P., & Agliardi, F. (2013). Deep seated gravitational slope deformations in the European Alps. *Tectonophysics, 605,* 13–33.

Dawson, A. G., Dawson, S., & Bondevik, S. (2006). A Late Holocene Tsunami at Basta Voe, Yell, Shetland Isles. *Scottish Geographical Journal, 122,* 100–108.

Dawson, A. G., Long, D., & Smith, D.E. (1988). The Storegga Slides: evidence from eastern Scotland for a possible tsunami. *Marine Geology, 82,* 271–276.

Dawson, S. & Smith, D. E. (1997). Holocene Relative Sea Level Changes on the margin of a glacio-isostatically uplifted area: an example from northern Caithness, Scotland. *The Holocene*, *7,* 59–77.

Dawson S. & Wickham-Jones C. R. (2007). Sea-level change and the prehistory of Orkney. *Antiquity*, *81,* 312.

Dick, R. (2015). *The tsunamigenic potential of rock-slope failures in a coastal setting as a possible source mechanism for the mid- or later Holocene tsunamis in Shetland.* Unpublished MSc thesis, University of Dundee.

Fabel, D., Ballantyne, C. K., & Xu, S. (2012). Trimlines, blockfields, mountain-top erratics and the vertical dimensions of the last British-Irish Ice Sheet in NW Scotland. *Quaternary Science Reviews, 55,* 91–102.

Firth, C. R., & Stewart, I. S. (2000). Postglacial tectonics of the Scottish glacio-isostatic uplift centre. *Quaternary Science Reviews, 19,* 1469–1493.

Flinn, D. (1964). Coastal and submarine features around the Shetland Isles. *Proceedings of the Geologists' Association, 75,* 321–340.

Flinn, D. (1969). On the development of coastal profiles in the north of Scotland, Orkney and Shetland. *Scottish Journal of Geology, 5,* 393–399.

Flinn, D. (1974). The coastline of Shetland. In R. Goodier (Ed.) *The Natural Environment of Shetland* (pp. 13–23). Swindon: Nature Conservancy Council.

Flinn, D. (1977). The erosion history of Shetland: a review. *Proceedings of the Geologists' Association*, *88,* 129–146.

Flinn, D. (1978). The most recent glaciation of the Orkney-Shetland channel and adjacent regions. *Scottish Journal of Geology, 14,* 109–123.

Flinn, D. (2009). The omission of conflicting evidence from the paper by Golledge et al. (2008). *Geografiska Annaler, 91A,* 253–256.

Flinn, D. (2014). *Geology of Unst and Fetlar in Shetland.* Memoir for 1:50 000 geological sheet 131 (Scotland). Keyworth: British Geological Survey.

Godard, A. (1965). *Récherches de Géomorphologie en Écosse du Nord-Ouest.* Paris: Masson.

Hall, A. M. (2013). The last glaciation of Shetland: local ice cap or invasive ice sheet? *Norwegian Journal of Geology, 93,* 229–242.

Hall, A. M., Hansom, J. D., & Jarvis, J. (2007). Patterns and rates of erosion produced by high energy wave processes on hard rock headlands: The Grind of the Navir, Shetland, Scotland. *Marine Geology, 248,* 28–46.

Hall, A. M., Hansom, J. D., Williams, D. M., & Jarvis. J. (2006). Distribution, geomorphology and lithofacies of cliff-top storm deposits: examples from the high-energy coasts of Scotland and Ireland. *Marine Geology, 232,* 131–155.

Hansom J. D., & Hall, A. M. (2009). Magnitude and frequency of extra-tropical North Atlantic cyclones: a chronology from cliff-top storm deposits. *Quaternary International, 195,* 45–52.

Hapke, C. J., & Richmond, B. M. (2002). The impact of climatic and seismic events on the short-term evolution of seacliffs based on 3-D mapping: northern Monterey Bay, California. *Marine Geology, 187,* 259–278.

Hinchliffe, S., & Ballantyne, C. K. (1999). Talus accumulation and rockwall retreat, Trotternish, Isle of Skye, Scotland. *Scottish Geographical Journal, 115,* 53–70.

Hinchliffe, S., & Ballantyne, C. K. (2009). Talus structure and evolution on sandstone mountains in NW Scotland. *The Holocene, 19,* 471–480.

Holmes, G. (1984). *Rock Slope Failure in Parts of the Scottish Highlands.* Unpublished PhD thesis, University of Edinburgh.

Hutchinson, J. N., Bromhead, E. N., & Chandler, M. P. (1991). Investigations of landslides at St Catherine's Point, Isle of Wight. In R. J. Chandler (Ed.) *Slope Stability Engineering: Developments and Applications* (pp. 169–178). London: Institute of Civil Engineers.

Jarman, D. (2006). Large rock-slope failures in the Highlands of Scotland: characterization, causes and spatial distribution. *Engineering Geology, 83,* 161–182.

Jarman, D. (2007). Introduction to the mass movements in the older mountain areas of Great Britain. In R. G. Cooper (Ed.) *Mass movements in Great Britain* (pp. 33–56). Geological Conservation Review Series No. 33. Peterborough: Joint Nature Conservation Committee.

Jones, D. K., & Lee, E. M. (1974). *Landsliding in Great Britain.* London: HMSO.

Jordan, J. T., Smith, D. E., Dawson, S. & Dawson, A. G. (2010). Holocene relative sea level changes in Harris, Outer Hebrides, Scotland, UK. *Journal of Quaternary Science*, *25,* 115–134.

Kline, S. W., Adams, P. N., & Limber, P. W. (2014). The unsteady nature of sea cliff retreat due to mechanical abrasion, failure and comminution feedbacks. *Geomorphology, 219,* 53–67.

Komar, P. D., & Shih, S. M. (1993). Cliff erosion along the Oregon coast: a tectonic sea level imprint plus local controls by beach processes. *Journal of Coastal Research, 9,* 747–765.

Lambe, T. W., & Whitman, R. V. (1969). *Soil Mechanics.* Chichester: Wiley.

Lee, G. W. (1920). *The Mesozoic rocks of Applecross, Raasay and NE Skye.* Memoir of the Geological Survey, Scotland. Edinburgh: British Geological Survey.

Lim, M., Rosser, N. J., Allison, R. J., & Petley, D. N. (2010). Erosional processes in the hard rock coastal cliffs at Staithes, North Yorkshire. *Geomorphology, 114,* 12–21.

Marrero, S. M., Phillips, F. M., Borchers, B., Lifton, N., Aumer, R. & Balco, G. (2016). Cosmogenic nuclide systematics and the CRONUScalc program. *Quaternary Geochronology, 31,* 160–187.

May, V. J., & Hansom, J. D. (2003). *Coastal Geomorphology of Great Britain.* Geological Conservation Review, Joint Nature Conservancy Council. Norwich: HMSO.

Mykura, W. (1976). *British Regional Geology: Orkney and Shetland.* Edinburgh: HMSO.

Mykura, W. & Phemister, J. (1976). *The Geology of Western Shetland.* London: HMSO.

Nishiizimui, K., Imamura, M., Caffee, M. W., Southon, J. R., Finkel, R. C. & McAninch, J. (2007). Absolute calibration of 10Be AMS standards. *Nuclear Instruments and Methods in Physics Research Section B: Beam Interaction with Materials and Atoms, 258,* 403–413.

Pánek, T., Lenart, J., Hradecky, J., Hercman, H., Braucher, R., Silhán, K. & Skarpich, V. (2018). Coastal cliffs, rock-slope failures and Late Quaternary transgressions of the Black Sea along southern Crimea. *Quaternary Science Reviews, 181,* 76–92.

Richards, A. (1971). *The evolution of marine cliffs and related landforms in the Inner Hebrides.* Unpublished PhD thesis, University of Wales at Aberystwyth.

Saintot, A., Henderson, I.H.C., & Derron, M-H. (2011). Inheritance of ductile and brittle structures in the development of large rock slope instabilities: examples from western Norway. *Geological Society, London, Special Publications, 351,* 27–78.

Shennan, I., & Horton, B. P. (2002). Holocene land- and sea-level changes around Great Britain. *Journal of Quaternary Science, 17,* 511–526.

Sunamara, T. (1992). *The Geomorphology of Rocky Coasts.* Chichester: Wiley.

Sverdrup, K. A. (2006) *Fundamentals of Oceanography.* 5th Edition. New York: McGraw-Hill.

Trenhaile, A. S. (1987). *The Geomorphology of Rock Slopes.* Oxford: Oxford University Press.

Trenhaile, A. S. (2002a). Rock coasts, with particular emphasis on shore platforms. *Geomorphology*, *48,* 7–22.

Trenhaile, A. S. (2002b). Modelling the Quaternary evolution of marine terraces on tectonically mobile rock coasts. *Marine Geology, 185,* 341–361.

Trenhaile, A. S. (2010). The effect of Holocene changes in relative sea level on the morphology of rocky coasts. *Geomorphology, 114,* 30–41.

Watters, R. J. (1972). *Slope stability in the metamorphic rocks of the Scottish Highlands,* Unpublished PhD thesis, University of London.

Williams, A. T., Davies, B., & Bomboe, P. (1993) Geometrical simulation studies of coastal cliff failures in Liassic strata, south Wales, U.K. *Earth Surface Processes and Landforms, 18,* 703–720.

Worth, D. H. (1956). *Some aspects of the geomorphology of the Isle of Arran.* Unpublished MSc thesis, University of London.

Captions to Figures

Figure 1 Location and generalized geology of Shetland.

Figure 2 Preliminary sea-level curve for Shetland (grey band), constrained by radiocarbon dates. Adapted from Bondevik *et al.* (2005) and reproduced with permission from Elsevier.

Figure 3 Google Earth™ oblique images of coastal landslides in metasedimentary rocks on Shetland. (a) Ler Wick landslide, Yell [HU 442922] showing the headscarp, large displaced blocks and fringe of large boulders at the slope foot. Fresh debris below the central gully indicates recent cliff collapse. (b) South Floin landslide complex, Yell [HU 455960] showing three or four conjoint headscarps, displaced blocks, basal fringe of landslide debris and scarplets extending 110 m inland from the cliff crest. (c) Saito landslide, NW Unst [HP 596157]; the light-tone of the headscarp and the freshly detached blocks at the cliff crest indicate recent slope failure. (d) Pund of Grevasand landslides, Ness of Hillswick, NW Mainland [HU 270757], illustrating tension cracks at and inland from the cliff crest, slipped blocks and large blocks deposited in the nearshore zone.

Figure 4 Distribution of coastal landslides ≥ 50 m wide in Shetland. Each dot represents either a single landside or a complex of up to five slide scars with conjoint headscarps. The absence of coastal landslides in central Mainland reflects a lack of cliffs > 30 m high.

Figure 5 Width to height relationships for individual landslides seated on metasedimentary rocks. Landslide complexes are excluded. Translational rockslides exhibit a moderate positive relationship between width and height, but deep-seated failures (squares) are generally much larger than other landslides.

Figure 6 Frequency of landslides plotted against aspect. Landslides occur on all aspects, but westerly aspects dominate.

Figure 7 Google Earth™ images of the west Fetlar coastal landslides. (a) Landslides F2–F7. F2 is classified as a complex DSGSD. F4–F7 are typical translational failures, with arcuate or cuspate headscarps displaced blocks and localized evidence of recent rockfall or erosion. (b) Landslides F12–F16. F13 and F16 are classified as DSGSDs; both exhibit recent frontal erosion.

F12 and F14 are translational rockslides. F15 is a landslide complex with evidence of recent localized rockfall and slope failure.

Figure 8 Geomorphology of the coastal landslides of west Fetlar.

Figure 9 (a) Site F1, showing the northern sidescarp and failure plane of an offshore-terminating translational failure, and seaward dip of principal joints. (b) Site F2 viewed from the SE, showing displaced blocks dipping gently seaward. The headscarp extends ~120 m from the crest of the cliff, indicating deep-seated failure. (c) Site F5, showing a recent rockfall sourced from a displaced landslide block. (d) Site F7, showing the degraded, partly-vegetated arcuate headscarp and two prominent displaced blocks. (e) Headscarp of site F8 (foreground), beyond which is a recent rockfall. In the background is the arcuate headscarp and displaced blocks of site F10. (f) Subdued, peat-filled trenches marking the sites of tension cracks at the rear of Site 13. These trenches and similar features at site F16 occur ~110-130 m from the cliff crest, and indicate limited deep-seated seaward shift of large rock masses.

Figure 10 Sampling sites for ^{10}Be exposure dating near the foot of the headscarp at site F8. (a) Sample F8.1, from rock protrusion left of the hammer. (b) Sample F8.2, from near the foot of a buttress; chisel (circled) rests on sample location.

Figure 11 Schematic sequence of landslide evolution on the west Fetlar coastline. (a) Early Holocene: antecedent rock slope and basal talus; sea level is depicted below the level of the slope foot. (b) Mid-Late Holocene: rising sea level allows wave action to erode the basal talus and the slope foot, triggering failure along steeply-dipping structural discontinuities. (c) Late Holocene: instability propagates upslope causing translational sliding of blocks on the upper slope. (d) Present: detached and slipped blocks occupy upper slope, and an actively-eroding face (at some sites) surmounts a structurally-controlled bedrock ramp.

Figure 12 Schematic depiction of the increased seaward curvature of principal stress, and alignment of a potential curved shear plane. Steepening of the antecedent slope (from AB to AC) or retreat of the antecedent slope (from AB to DC) debuttresses the rock mass farther inland and increases the average gradient of the potential shear plane. Both effects may instigate deep-seated displacement of rock over 100 m inland from the slope crest.

Table 1 Recorded landslide frequency on different lithologies

Lithology:	Metasedimentary rocks	Granitic rocks	Sandstones	Ophiolite complex	Basement gneiss	Volcanic rocks
Recorded landslides[1]:	92	16	10	8	2	0
Percentage:	71.9	12.5	7.8	6.2	1.6	0.0
Cliffs > 30m high (%)	48.9	21.3	14.8	9.4	2.0	3.6

[1] Recorded landslides (n = 128) includes individual sites, landslide complexes and DSGSDs

Table 2 Sample location and ^{10}Be analytical data

Sample	OS Grid Reference	Latitude (°N)	Longitude (°W)	Altitude m OD	Sample thickness mm	Sample density g cm^{-3}	Shielding factor[a]	[^{10}Be][b] atom g^{-1}
F4 landslide								
F4-1	HU58959090	60.597	0.925	75	21	2.65	0.496	9777±503
F4-2	HU58959090	60.597	0.925	70	24	2.65	0.496	10007±533
F8 landslide								
F8-1	HU59169040	60.593	0.922	58	23	2.67	0.638	13421±558
F8-2	HU59169040	60.593	0.922	61	22	2.66	0.638	13426±1143

[a] Calculated using the online exposure age calculators formerly known as the CRONUS-Earth online exposure age calculators (Balco et al. 2008).

[b] Normalised to the '07KNSTD' standardization of Nishiizumi et al. (2007) and corrected for a procedural chemistry background of 49630±9596 ^{10}Be atoms. Uncertainties (±1σ) include all known sources of analytical error.

Table 3 ^{10}Be exposure ages

Sample	AMS ID	LLPR, Lm scaling			CRONUScalc, Lm scaling		
		Exposure age (years)	Internal uncertainty (years)	External uncertainty (years)	Exposure age (years)	Internal uncertainty (years)	External uncertainty (years)
Fetlar 4 rockslide							
F4-1	b9702	4366	226	249	4410	228	410
F4-2	b9705	4533	241	264	4580	244	430
F4 weighted mean		4444	165	196	4489	167	385
Fetlar 8 rockslide							
F8-1	b9749	4792	200	231	4810	201	430
F8-2	b100110	4774	409	424	4790	410	560
F8 weighted mean		4789	180	213	4806	180	422

Internal uncertainties (±1σ) reflect analytical uncertainties on sample processing and ^{10}Be measurements. External uncertainties (±1σ) incorporate in addition uncertainties in the calibration and scaling procedure. Calculated exposure ages assume a post-exposure erosion rate (ε) of 1 mm ka^{-1}. Calculation of ages for zero erosion (ε = 0) reduces the above ages by <0.4% and calculation for ε = 2 mm ka^{-1} increases the above ages by <0.4%.

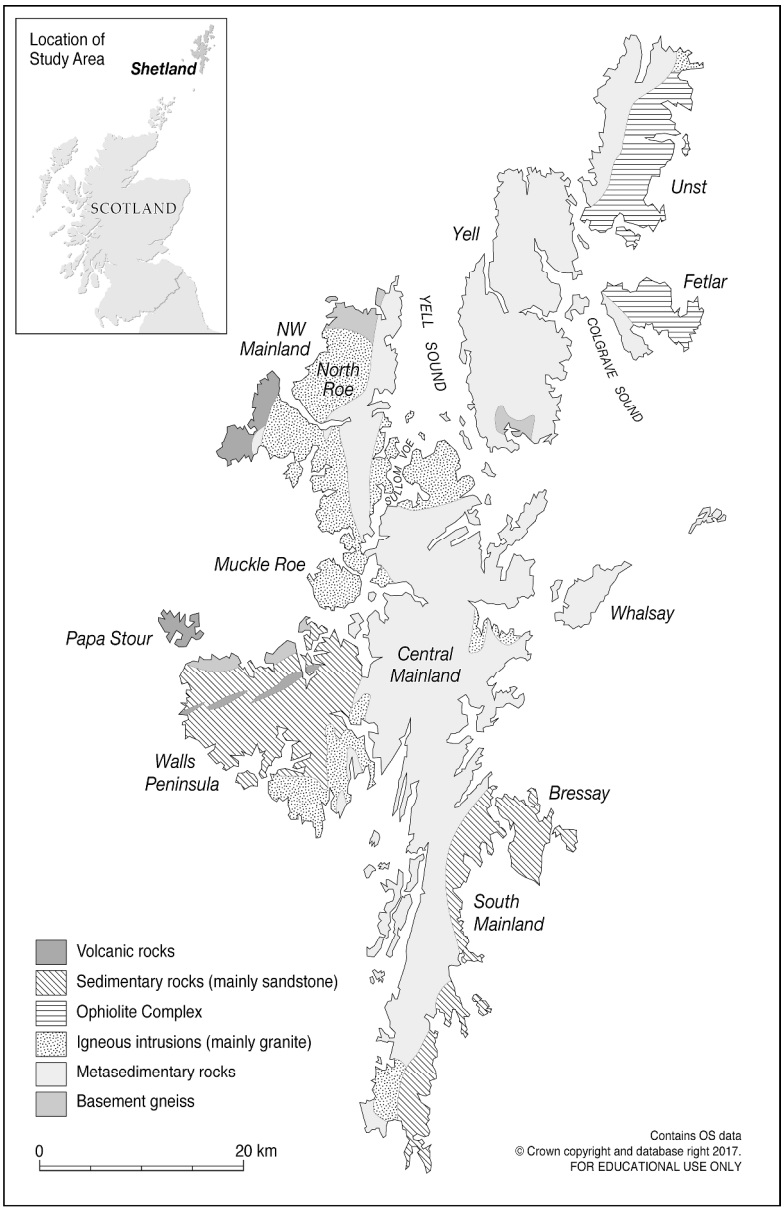

Figure 1 Location and generalized geology of Shetland.

163x252mm (600 x 600 DPI)

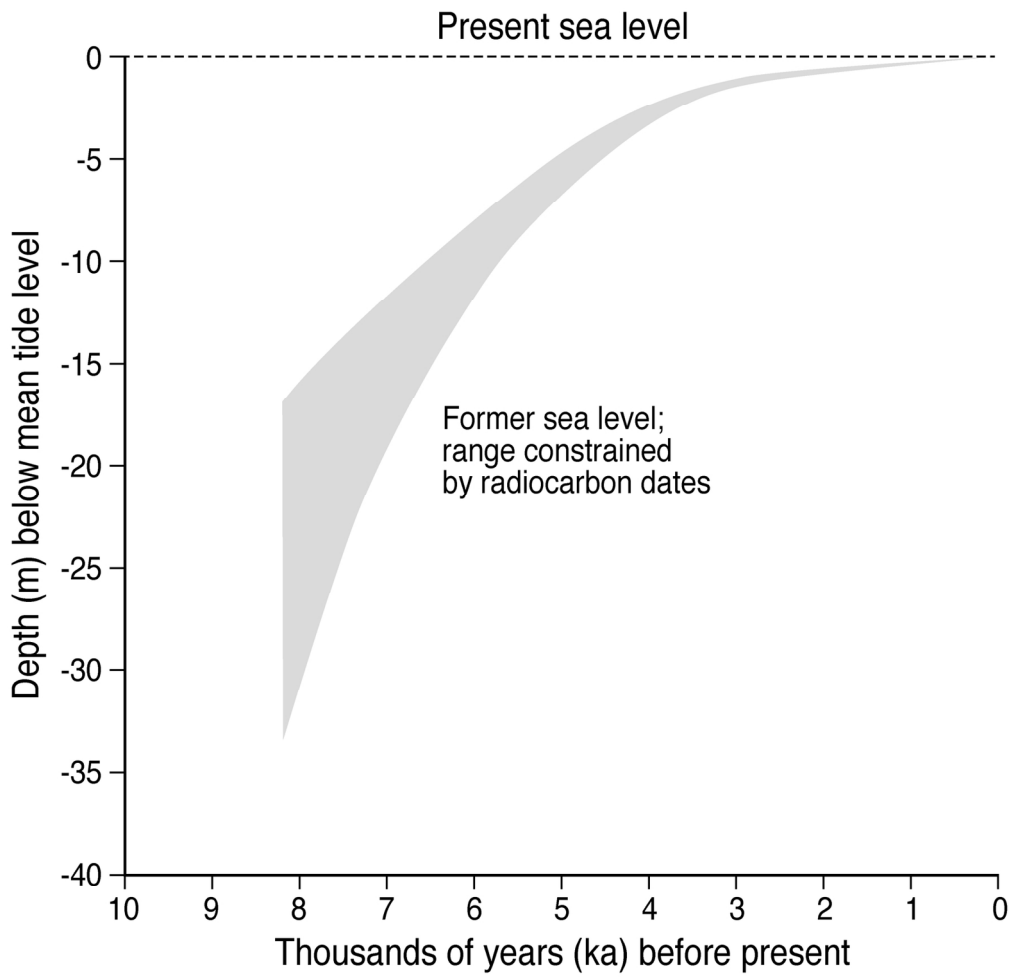

Figure 2 Preliminary sea-level curve for Shetland (grey band), constrained by radiocarbon dates. Adapted from Bondevik et al. (2005) and reproduced with permission from Elsevier.

75x73mm (600 x 600 DPI)

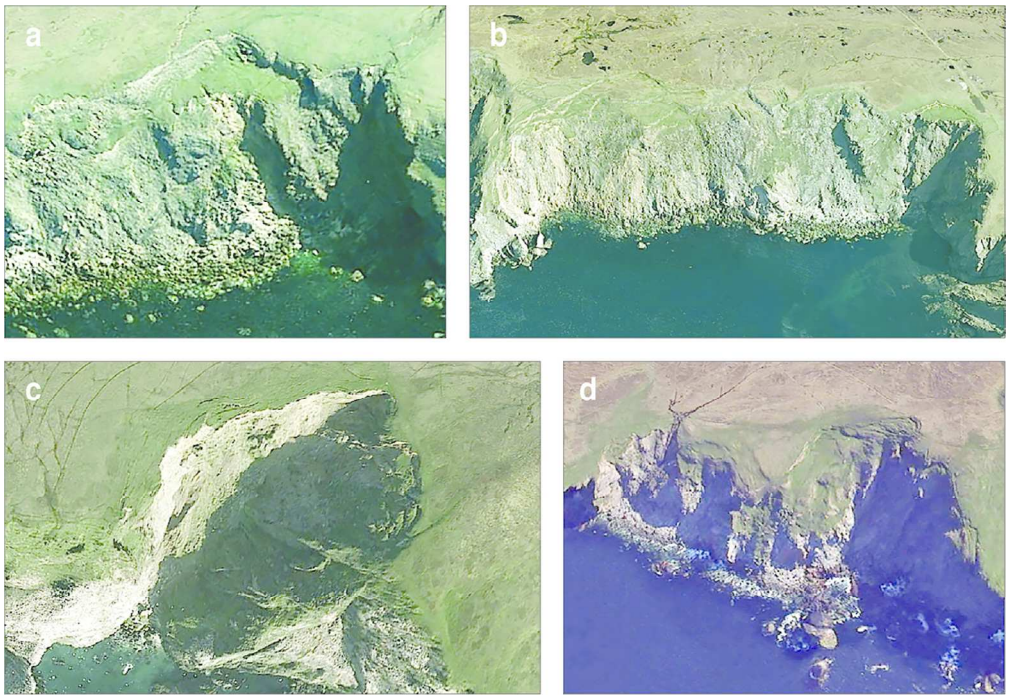

Figure 3 Google EarthTM oblique images of coastal landslides in metasedimentary rocks on Shetland. (a) Ler Wick landslide, Yell [HU 442922] showing the headscarp, large displaced blocks and fringe of large boulders at the slope foot. Fresh debris below the central gully indicates recent cliff collapse. (b) South Floin landslide complex, Yell [HU 455960] showing three or four conjoint headscarps, displaced blocks, basal fringe of landslide debris and scarplets extending 110 m inland from the cliff crest. (c) Saito landslide, NW Unst [HP 596157]; the light-tone of the headscarp and the freshly detached blocks at the cliff crest indicate recent slope failure. (d) Pund of Grevasand landslides, Ness of Hillswick, NW Mainland [HU 270757], illustrating tension cracks at and inland from the cliff crest, slipped blocks and large blocks deposited in the nearshore zone.

128x88mm (300 x 300 DPI)

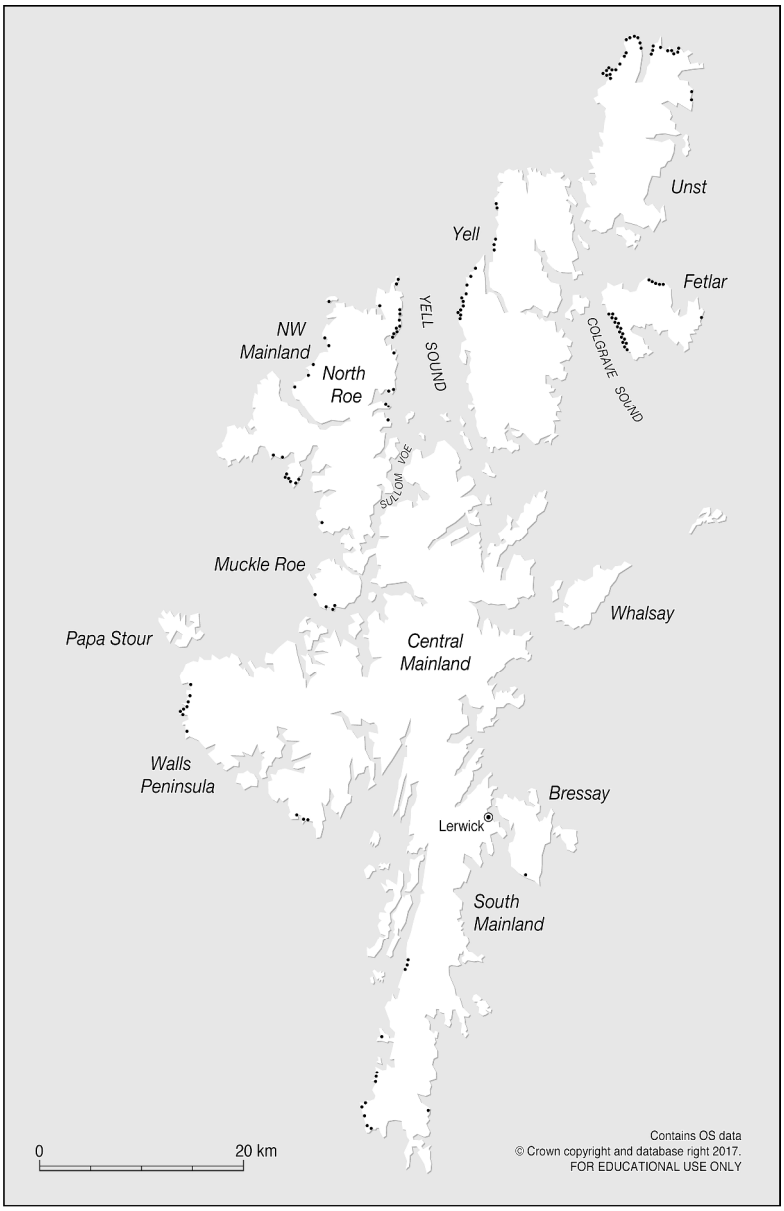

Figure 4 Distribution of coastal landslides ≥ 50 m wide in Shetland. Each dot represents either a single landside or a complex of up to five slide scars with conjoint headscarps. The absence of coastal landslides in central Mainland reflects a lack of cliffs > 30 m high.

163x252mm (600 x 600 DPI)

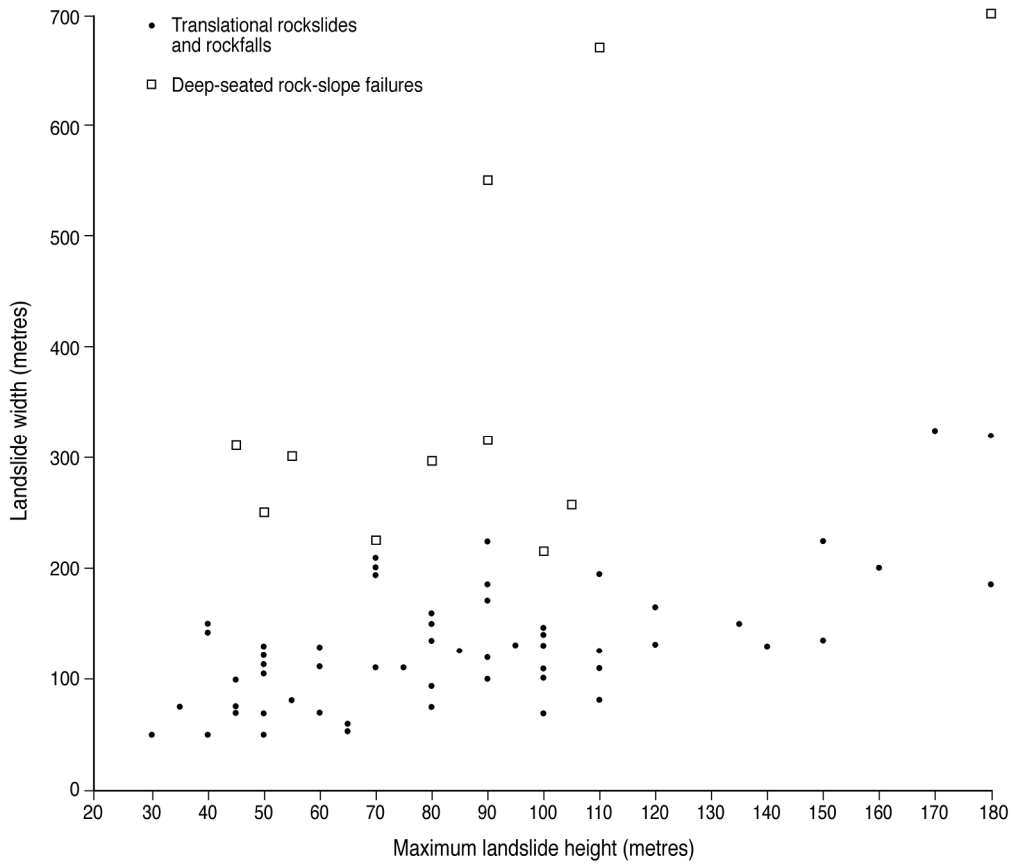

Figure 5 Width to height relationships for individual landslides seated on metasedimentary rocks. Landslide complexes are excluded. Translational rockslides exhibit a moderate positive relationship between width and height, but deep-seated failures (squares) are generally much larger than other landslides.

107x92mm (600 x 600 DPI)

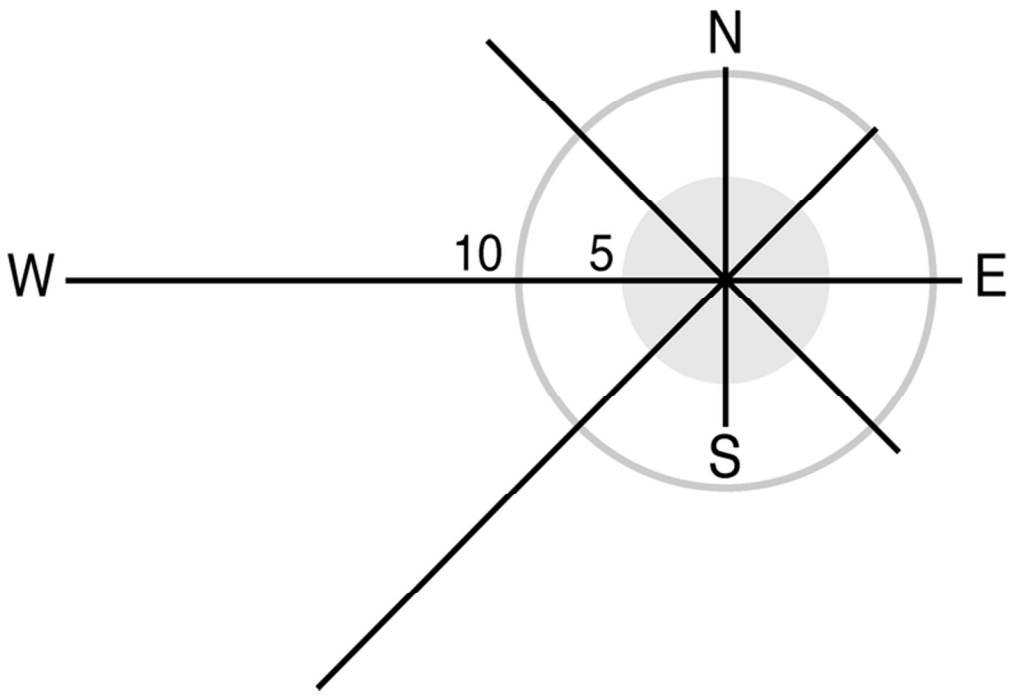

Figure 6 Frequency of landslides plotted against aspect. Landslides occur on all aspects, but westerly aspects dominate.

33x22mm (600 x 600 DPI)

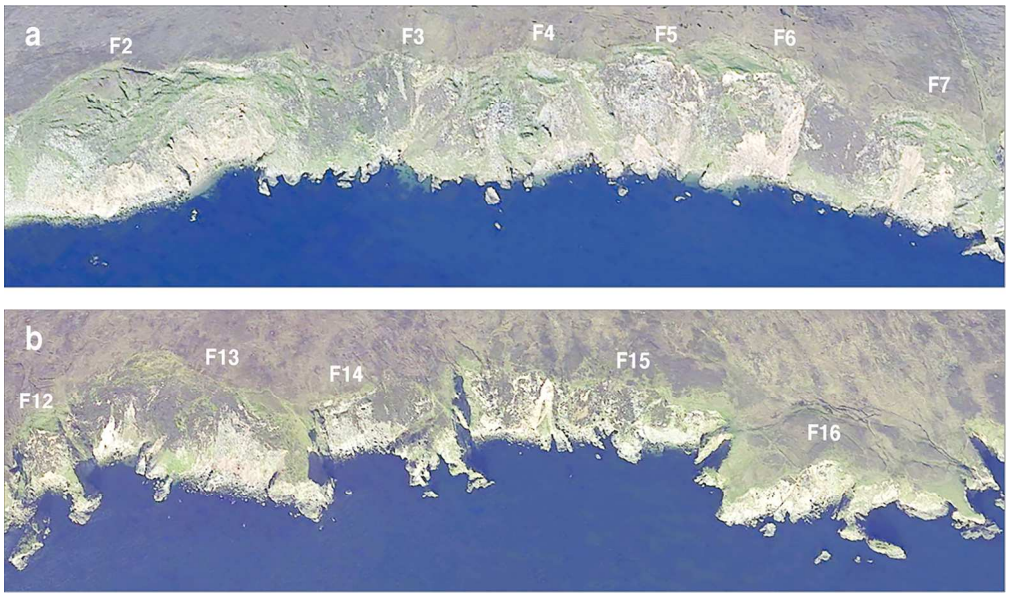

Figure 7 Google EarthTM images of the west Fetlar coastal landslides. (a) Landslides F2–F7. F2 is classified as a complex DSGSD. F4–F7 are typical translational failures, with arcuate or cuspate headscarps displaced blocks and localized evidence of recent rockfall or erosion. (b) Landslides F12–F16. F13 and F16 are classified as DSGSDs; both exhibit recent frontal erosion. F12 and F14 are translational rockslides. F15 is a landslide complex with evidence of recent localized rockfall and slope failure.

128x75mm (300 x 300 DPI)

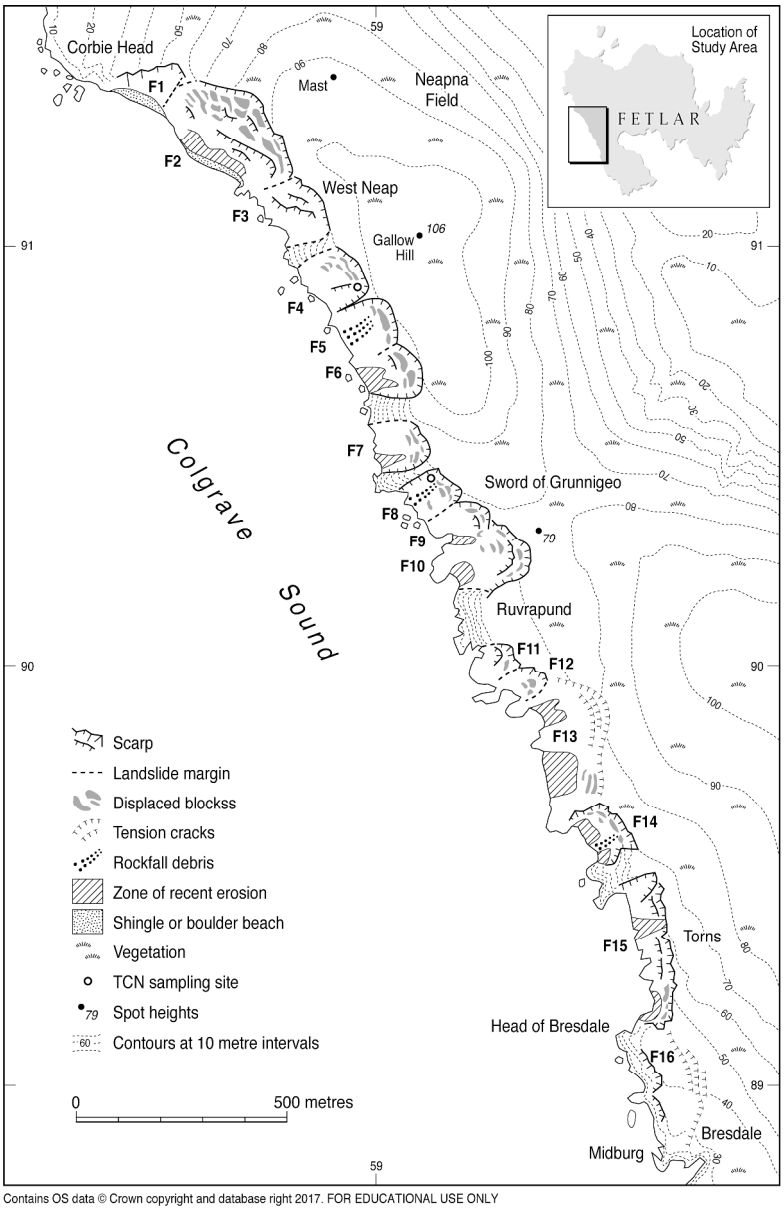

Figure 8 Geomorphology of the coastal landslides of west Fetlar.

163x251mm (600 x 600 DPI)

Figure 9 (a) Site F1, showing the northern sidescarp and failure plane of an offshore-terminating translational failure, and seaward dip of principal joints. (b) Site F2 viewed from the SE, showing displaced blocks dipping gently seaward. The headscarp extends ~120 m from the crest of the cliff, indicating deep-seated failure. (c) Site F5, showing a recent rockfall sourced from a displaced landslide block. (d) Site F7, showing the degraded, partly-vegetated arcuate headscarp and two prominent displaced blocks. (e) Headscarp of site F8 (foreground), beyond which is a recent rockfall. In the background is the arcuate headscarp and displaced blocks of site F10. (f) Subdued, peat-filled trenches marking the sites of tension cracks at the rear of Site 13. These trenches and similar features at site F16 occur ~110-130 m from the cliff crest, and indicate limited deep-seated seaward shift of large rock masses.

128x147mm (300 x 300 DPI)

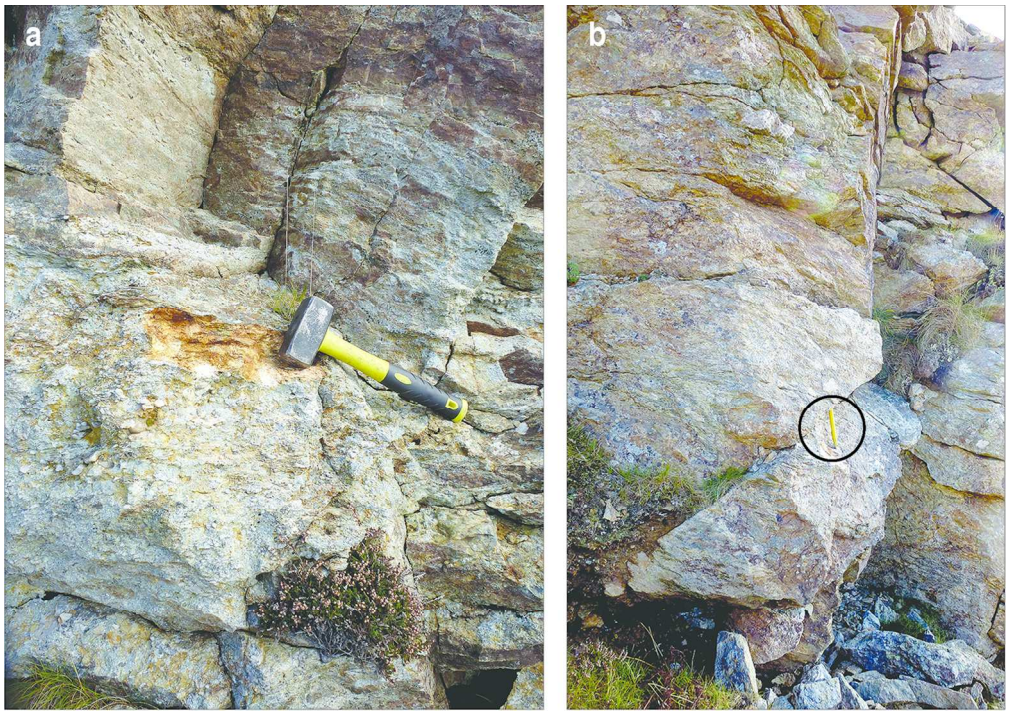

Figure 10 Sampling sites for 10Be exposure dating near the foot of the headscarp at site F8. (a) Sample F8.1, from rock protrusion left of the hammer. (b) Sample F8.2, from near the foot of a buttress; chisel (circled) rests on sample location.

128x90mm (300 x 300 DPI)

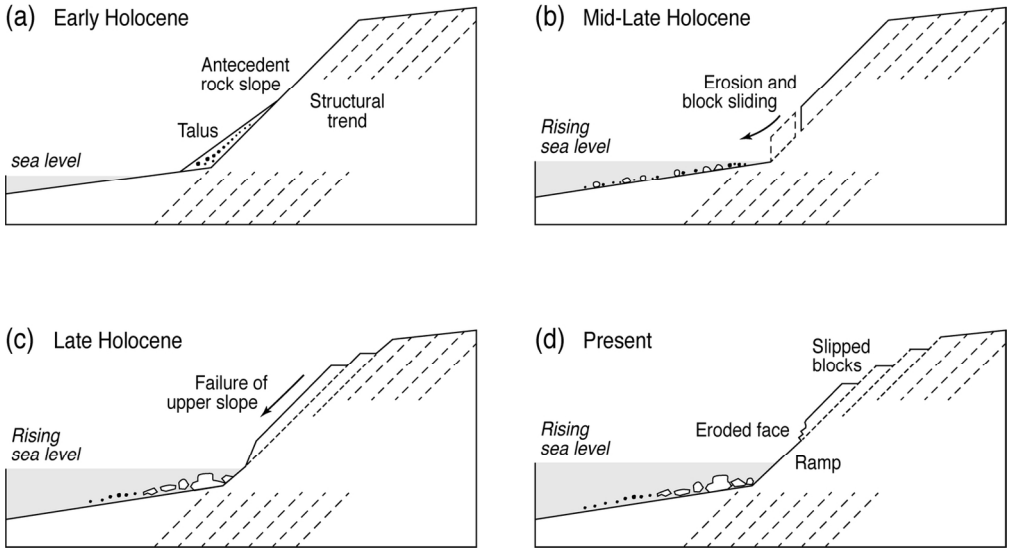

Figure 11 Schematic sequence of landslide evolution on the west Fetlar coastline. (a) Early Holocene: antecedent rock slope and basal talus; sea level is depicted below the level of the slope foot. (b) Mid-Late Holocene: rising sea level allows wave action to erode the basal talus and the slope foot, triggering failure along steeply-dipping structural discontinuities. (c) Late Holocene: instability propagates upslope causing translational sliding of blocks on the upper slope. (d) Present: detached and slipped blocks occupy upper slope, and an actively-eroding face (at some sites) surmounts a structurally-controlled bedrock ramp.

70x38mm (600 x 600 DPI)

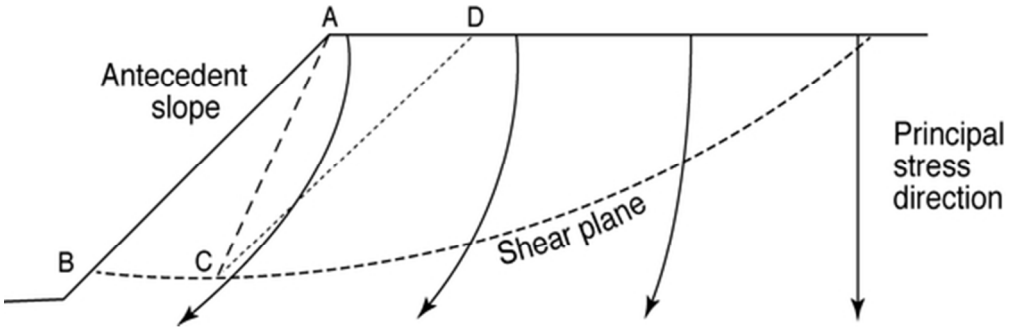

Figure 12 Schematic depiction of the increased seaward curvature of principal stress, and alignment of a potential curved shear plane. Steepening of the antecedent slope (from AB to AC) or retreat of the antecedent slope (from AB to DC) debuttresses the rock mass farther inland and increases the average gradient of the potential shear plane. Both effects may instigate deep-seated displacement of rock over 100 m inland from the slope crest.

24x8mm (600 x 600 DPI)